THE JOURNAL OF PHYSICAL CHEMISTRY B

Article

pubs.acs.org/JPCB

Catalysis of Dioxygen Reduction by *Thermus thermophilus* Strain HB27 Laccase on Ketjen Black Electrodes

Peter Agbo, James R. Heath, and Harry B. Gray*

California Institute of Technology, Pasadena, California

Supporting Information

ABSTRACT: We present electrochemical analyses of the catalysis of dioxygen reduction by *Thermus thermophilus* strain HB27 laccase on ketjen black substrates. Our cathodes reliably produce 0.56 mA cm^{-2} at 0.0 V vs AgIAgCl reference at 30 °C in air-saturated buffer, under conditions of nonlimiting O_2 flux. We report the electrochemical activity of this laccase as a function of temperature, pH, time, and the efficiency of its conversion of dioxygen to water. We have measured the surface concentration of electrochemically active species, permitting the extraction of electron transfer rates at the enzyme-electrode interface: 1 s^{-1} for this process at zero driving force at 30 °C and a limiting rate of 23 s^{-1} at 240 mV overpotential at 50 °C.

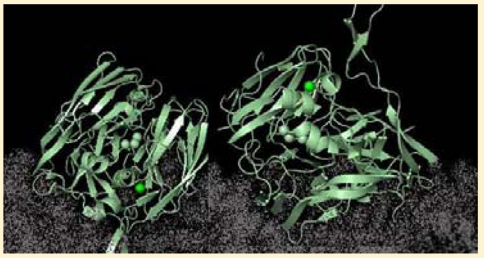

INTRODUCTION

Fuel cells remain one of the most promising modes of utilizing hydrogen or methanol by coupling their oxidation at anodic surfaces to the four-electron reduction of dioxygen to water at the cathode. In general, the cathodic transformation of dioxygen to water proves limiting to current production (and therefore power output) in fuel cells.[1] While kinetic limitations may be overcome by employing platinum on carbon (Pt/C) catalysis at the cathode, this is not a viable, long-term solution as a consequence of the high cost of platinum.[2] In biochemical approaches to this problem, the multicopper oxidases (MCOs) have proven to be a good starting point. These enzymes, comprised of either two or three cupredoxin domains that ligate copper ions at type 1 and type 2/3 centers, have evolved as efficient dioxygen reductases, capable of coupling the oxidation of phenols and other organic substrates to the reduction of O_2 to form H_2O.[3] Electron flow through these proteins proceeds in a stepwise fashion, with a reduced substrate donating charge to the type 1 center, followed by long-range electron transfer to the type 2/3 trinuclear copper cluster where dioxygen reduction occurs.[3−6]

We are working with an MCO from *Thermus thermophilus* strain HB27, an isoform of the multicopper oxidase subset known as laccases. The reported thermostability of this MCO makes it a promising candidate for operation in fuel cells, with a half-life of 14 h at 80 °C and a catalytic optimum at 95 °C in solution.[7] To date, characterization of *T. thermophilus* laccase has been limited to either biochemical assays of the enzyme's catalytic turnover of substrates in solution or homogeneous electrochemical measurements in the presence of the small-molecule mediator 2,2′-azino-bis(3-ethylbenzothiazoline-6-sulfonic) acid (ABTS).[7,8] As a complement to such work, we performed a comprehensive study of the electrochemical activity of *T. thermophilus* laccase with the enzyme functioning as a heterogeneous catalyst without a redox mediator. Our choice of catalytic support was inspired by previous studies where other MCOs, such as copper efflux oxidase (CueO), *Trametes versicolor* laccase, and *Streptomyces coelicor* laccase, were found to catalyze dioxygen reduction when adsorbed on ketjen black, a carbon substrate that has a very high specific (BET) surface area due to its porosity (Figure 1).[9−13]

While past work in protein electrochemistry has explored the utility of other electrode materials such as anthracene-modified gold and surfaces modified with self-assembled alkyl monolayers (SAMs), these electrodes are not realistic options for cathodes intended for practical fuel cell applications because of their lengthy fabrication times and relative fragility. Conductive carbon powders such as ketjen black represent cheap, robust surfaces that are readily processed into electrode assemblies for electrochemical testing. Perhaps the most compelling reason to employ these materials in protein electrochemistry derives from the existing precedent for the use of carbon blacks in fuel cell membrane-electrode assemblies (MEAs), making ketjen black supports a logical starting point for investigations of heterogeneous catalysis by *Thermus thermophilus* strain HB27 laccase.

EXPERIMENTAL SECTION

Cloning. The gene for wild type *T. thermophilus* laccase was amplified from a nonexpression vector using the following primers: 5′GATCCgcggaacgcccgaccctgccgattccggatctgc-3′ (Forward), 5′AATTCcacggtaaagcccagcatcatgccggtatcttcatg-3′ (Reverse). Capitalized regions in the primers denote restriction sites that were used for cloning into plasmids (BamH1, EcoR1). PCR amplification of the wild-type gene was performed using the Expand High Fidelity PCR system (Roche). Spurious

Received: October 2, 2012
Revised: November 7, 2012

   dx.doi.org/10.1021/jp309759g | *J. Phys. Chem. B* XXXX, XXX, XXX−XXX

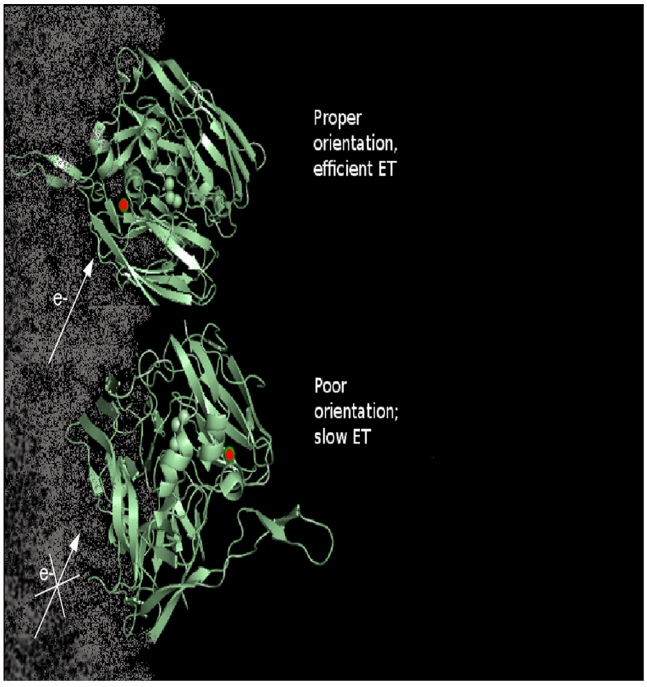

Figure 1. Orientations representing one of two possible extremes when laccase (PDB ID: 2XU9) is adsorbed onto a ketjen black substrate: (top) The protein is adsorbed with the type 1 copper center (shown in red) held near the electrode surface, allowing for rapid interfacial ET. (bottom) Enzyme adsorption occurs such that the type 1 center is held opposite the electrode surface, inhibiting charge transfer.

nucleic acid amplicons were cleaned from the PCR reaction using the Qiagen PCR Purification Kit. The gene was ligated into the pET22b(+) expression vector by separately digesting both the plasmid and gene insert using BamH1 and EcoR1 restriction enzymes in a single reaction, yielding hanging end restriction cuts for both the laccase gene insert and the pET22b(+) vector. Removal of residual nucleic acid fragments from the restriction cutting was also performed using the Qiagen PCR Purification Kit. The purified linear plasmid and gene insert were then mixed in 1:5 molar ratio and incubated in a reaction using T4 DNA ligase (Roche) at room temperature for 12 h, to allow insertion of the WT laccase gene into the pET vector. Novablue Singles cells (EMD Millipore Chemicals) were then transformed with the ligation reactions and plated on agar plates with LB media (BD) inoculated with 0.1 mg/mL ampicillin (Sigma). Colonies to be screened were then picked and grown in 5 mL cultures in LB broth for 16 h at 37 °C. A Qiagen miniprep kit was used to isolate plasmid DNA. Confirmation of successful cloning was performed both through diagnostic digests of plasmid DNA extracted from transformed cells and also through sequencing (Laragen Sequencing) using T7 promoter and T7 terminator sequencing primers.

Expression. Plasmid DNA cloned with the gene for laccase was transformed into *E. coli* Rosetta 2 (DE3) cell lines (EMD Millipore Chemicals). Low expression yields of laccase in standard BL21 (DE3) *E. coli*, caused by poor codon compatibility between our gene and typical *E. coli* tRNA expression profiles, mandated our use of Rosetta 2 (DE3) cell lines that overexpress tRNAs uncommon in *E. coli*. Transformed cells were grown in 6 L of autoclaved TB broth (47.6 g/L) amended with 0.1 mg/mL sodium ampicillin and 34 μg/mL chloramphenicol for 16 h at 37 °C and induced with 1 mM IPTG for an additional 5 h. Cells were then harvested by centrifugation and equilibrated against 20% sucrose, 1 mM EDTA, 300 mM Tris, pH 8.1 for one hour. After equilibration, the cells were repelleted by centrifugation at 7000 rpm for 25 min. Following removal of the supernatant, the cells were resuspended in pH 6 20 mM sodium acetate and then treated with lysozyme and DNase for 30 min. Extracts were sonicated for 10 min and then centrifuged for 1 h at 14000 rpm. Following centrifugation, the supernatant was carefully decanted into a clean container and stored overnight in a cold room.

Metalation. Incorporation of copper into the laccase apoenzyme was achieved by dropwise addition of 10 mM $CuSO_4$ to the crude extracts. Addition was continued until the extracts turned a dark green color. The metalated lysate was then stirred for at least an hour in a 4 °C cold room.

Chromatography. Following metalation, batch columns were run as initial purifications of the extracts. Crude lysates were loaded onto a CM Sepharose (cation exchange) column equilibrated with 3 column volumes of 100 mM sodium acetate, pH 6.0. Following the passage of nonbinding proteins through the column, bound proteins were eluted using 100 mM sodium acetate + 500 mM NaCl. Bound fractions were collected, pooled, and concentrated to a 15 mL volume using an Amicon with a 30 kDa molecular weight cutoff (MWCO) membrane.

Buffer exchange of the extract was then performed by using an FPLC desalting column (20 mL bed volume) equilibrated with 20 mM sodium acetate, pH 6.3. Immediately after desalting, cation exchange was performed using a HiTrap SP column equilibrated with pH 6.3, 20 mM sodium acetate and eluting in a 30% gradient of 1 M NaCl over 40 min. A final chromatographic separation by size was done using a Superdex 75 gel filtration column equilibrated in pH 6.0, 20 mM sodium acetate. Expression yields were quantified using the type 1 copper absorption at 610 nm ($\varepsilon \sim 5000\ M^{-1}\ cm^{-1}$). Enzyme purity was verified using SDS-PAGE and Matrix Assisted Laser Desorption Ionization − Time of Flight (MALDI-TOF) mass spectrometry (Supporting Information).

Circular Dichroism Spectroscopy (CD). CD wavelength scans and thermal denaturation characterization were performed by diluting protein samples so that absorbances at 280 nm were 0.2. Scans of protein samples were taken as a function of wavelength between 210 and 260 nm. To confirm that the purified enzyme was laccase and not wild-type CueO, an enzyme homologue (found in the *E. coli* genome) with a similar mass and virtually identical UV−vis spectrum to that of *Thermus thermophilus* laccase, titrations were performed by monitoring changes in ellipticity at 222 nm as a function of temperature between 18 and 95 °C (SI). CueO exhibits a sharp denaturing transition at 80 °C, whereas wild-type *T. thermophilus* laccase retains its structure at temperatures beyond 95 °C.[7]

Electrode Fabrication. Ketjen black (AkzoNobel) was used as received. Ketjen black slurries were prepared by first modifiying the carbon blacks with 1-pyrenebutyric acid (Sigma). This modification had the effect of reducing the electrode background, making anaerobic voltammetry more feasible. A 4.7 mg/mL solution of 1-pyrenebutyric acid was prepared in a solvent mixture of 70% acetone and 30% DMSO. Ketjen pellets were ground in a mortar. The ground ketjen black (60 mg) was then added to the 1-pyrene butyrate

dx.doi.org/10.1021/jp309759g | J. Phys. Chem. B XXXX, XXX, XXX−XXX

solution. The resulting colloid was vortexed briefly and then placed on a shaker in a cold room for 30 min to ensure saturation of the carbon black with the pyrene derivative. Adsorption isotherms generated by monitoring the 344 nm (pyrene) signature in the supernatant (ε = 41000 M^{-1} cm^{-1}) revealed an adsorption capacity of ca. 2.5 mg pyrene butyrate per mg ketjen black with the given solvent composition. The modified ketjen black was then collected by vacuum filtration. Electrode slurries using the modified carbon powders were made by adding 40 mg of ketjen black and 10 mg of polyvinylidene difluoride (PVDF, Sigma) to a scintillation vial with 5.0 mL of N-methyl-2-pyrrolidone (Sigma). The slurry was mixed by pipet and then sonicated for at least two hours to homogenize. Eight μL of the slurry was pipetted onto the surfaces of highly oriented pyrolytic graphite (HOPG, K-TEK Nanotechnology) electrodes that had been lightly abraded using emery paper and cut to dimensions of 0.5 × 0.5 cm. The electrodes were then dried in an oven at 60−70 °C for at least 12 h.

Polarization and RDE Experiments. Electrode polarization studies were performed in 20 mM sodium acetate, pH 5.0 in a 250 mL cell held at 30 °C. All potentials were referenced versus an Ag|AgCl electrode (CHI Instruments). The ketjen-black assembly served as the working electrode, while a platinum wire served as the counter electrode. Rotating disk electrode experiments were performed using a PINE Instruments rotator. Before these experiments, background scans were taken of each electrode at each speed examined in our tests. Following control scans, the electrode tips were immersed in 5 μM solutions of *T. thermophilus* laccase for two hours. During the immobilization process, electrodes were rotated at 100 rpm to mix. Following electrode functionalization with laccase, electrode surfaces were rinsed free of excess enzyme by brief immersion and gentle stirring in pH 5.0 20 mM sodium acetate. Anaerobic control measurements were performed by sparging the cell buffer with argon for at least 30 min prior to voltammetry. Linear sweep voltammetry (LSV) was performed by scanning electrodes from 0.6 to 0.0 V vs Ag|AgCl at 10 mV s^{-1}. We employed rotating disk electrode (RDE) analysis to discern the dependence of electrode activity on rates of dioxygen mass transport and also to determine an upper limit for the cathodic current produced by these electrodes in the absence of mass transport limitations.

Tafel Analysis. Tafel data were collected by scanning the electrodes anodically in aerated pH 5.0 20 mM sodium acetate while rotating at 3000 rpm between 0.0 and 0.6 V vs Ag|AgCl. Cathodic branches of the generated Tafel plots were used for fitting and extraction of the exchange current (i_0), charge transfer resistance (Ω_{ct}), Tafel slope, and transmission coefficient (α) of the system.[14] We fit these data to a low-overpotential limiting case of the Butler−Volmer equation, constraining the quantity $d\eta/di$ with respect to the exchange current (eq 1)[15]

$$d\eta/di = RTF^{-1}i_0^{-1} \tag{1}$$

where R is the ideal gas constant (8.31 J mol^{-1} K^{-1}), and T is the cell temperature, 303 K. In practice, data fitting was achieved by comparing the Tafel linear fit to the value of $d\eta/di$ yielded by a corresponding linear sweep voltammogram of an electrode. If the correct regime in the Tafel plot (the range of η) is chosen for a linear fit, the resulting exchange current should yield a value for $d\eta/di$ equal to that observed in a linear sweep of the electrode in the same voltage region. This method provided a systematic way to determine the appropriate range of overpotentials that were required for correct Tafel fitting. Using this procedure, our fits reliably yielded a $d\eta/di$ within 6% of the ideal value (for a given exchange current).

Faradaic Efficiency. Faradaic yields for O_2 conversion to H_2O by laccase were obtained by comparing the charge passed over the course of an experiment with the change in O_2 content of the cell. A five-port, 25 mL distillation flask filled with pH 5.0 20 mM sodium acetate served as the electrochemical cell. Prior to electrode operation, the reference electrode and FOXY O_2 sensor (Ocean Optics) were inserted into the ports of the distillation flask and secured with parafilm. The counter electrode was placed in a glass capillary with a fritted end that was filled with the cell buffer. The capillary was then mounted in a cell port and secured with parafilm. Two-point calibration using dissolved O_2 concentrations of 0% and 20.8% (atmospheric pO_2) was used to ready the probe before each experimental trial. A small magnetic stir bar was placed in the cell to allow for even mixing of dissolved dioxygen during experimental runs. Following calibration, a ketjen black working electrode modified with laccase, as described earlier, was fitted to the cell. Rubber gaskets were fitted over the electrode assembly to ensure an airtight seal. A 5.0 mL syringe filled with the cell buffer was attached to the fifth port. Any remaining air pockets in the cell were easily removed by depressing the syringe and filling the cell to its maximum volume. Following apparatus assembly, the dioxygen levels in the cell were allowed to stabilize for at least one hour. Once the baseline was established, a 0.0 V potential (vs Ag|AgCl) was applied to the working electrode, and the resulting current and changes in O_2 concentration were monitored for two hours. With gentle stirring, we were able to maintain a current of 25−30 μA during data acquisition. At the end of the experiment, we quantified the faradaic yield using (eq 2)

$$E = nF\frac{\nu\Delta[O_2]}{\int_0^t idt} \tag{2}$$

where E is the faradaic efficiency, n = 4 for dioxygen reduction to water, ν is the cell volume, $\Delta[O_2]$ is the change in the concentration of dioxygen during the experiment, F is Faraday's constant, and i is the current.

Temperature and pH Dependences. Titrations of laccase electrodes were conducted in pH 5.0 20 mM sodium acetate between 20 and 80 °C while rotating at 3200 rpm. Following cell equilibration at each temperature, the electrodes were inserted into the cell, and voltammograms were recorded at 10 mV s^{-1} between 0.0 and 0.6 V vs Ag|AgCl. Electrodes were immediately removed from the cell following completion of a scan to help minimize reduced electrode activity caused by any overexposure of the protein films to high temperatures. Studies of pH dependence were done at 18 °C in 20 mM sodium acetate at pH 2.90, 5.05, 6.04, 6.98, 8.06, and 9.16. Investigations of the pH dependence of the type 1 copper reduction potential were conducted at pH 4.00, 4.50, 5.00, 5.46, and 6.01.

Surface Concentration Measurements. Concentrations of active enzymes adsorbed to ketjen black were measured by cyclic voltammetry. Electrodes were functionalized with laccase as described before and then fitted to an airtight cell. The cell was placed in a copper mesh Faraday cage, with the working electrode grounded to the base of the cage. The cell buffer (pH 4.76 50 mM sodium phosphate + 250 mM sodium sulfate) was

dx.doi.org/10.1021/jp309759g | J. Phys. Chem. B XXXX, XXX, XXX−XXX

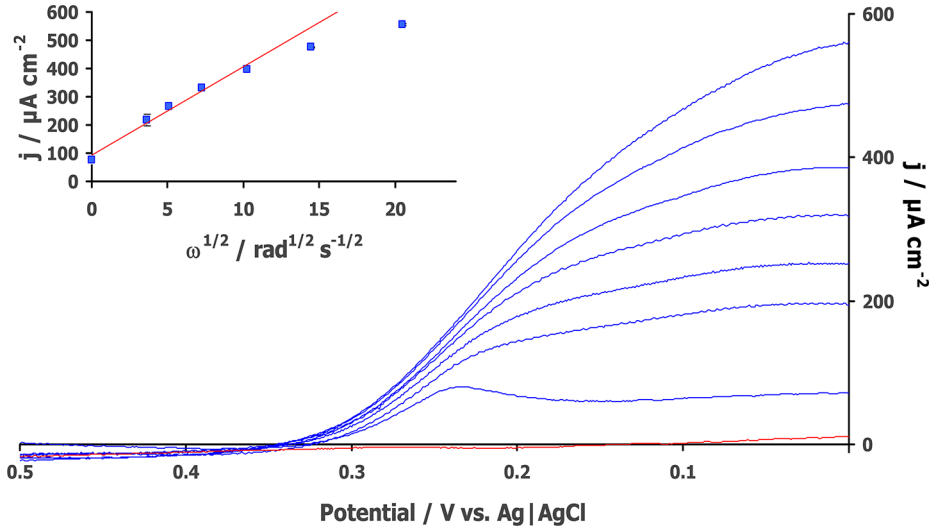

Figure 2. Cathodic polarization of electrodes comprised of laccase adsorbed onto modified ketjen black in pH 5.0, 20 mM sodium acetate buffer. Current onset is observed around 340 mV vs Ag|AgCl. Linear sweep voltammagrams of the electrodes demonstrate monotonic increases in the current as a function of rotation rate from 0 to 4000 rpm (blue traces). Electrodes show no activity in the absence of O_2 (red curve, Argon sparged media). Inset: peak current density as a function of rotation rate. Loss of the linear relationship between current density and $\omega^{1/2}$ begins around 2000 rpm as O_2 flux stops being rate limiting. Error bars are in black.

purged of dioxygen by vigorous sparging of the media with argon for one hour. To reduce the risk of any O_2 leakage into the cell, argon was pumped into the cell during the entire course of the experiment. After establishing an anoxic atmosphere, amperometric scans of the electrodes were performed to ensure all enzyme centers were oxidized. This was done by poising the electrodes at 0.6 V vs Ag|AgCl reference and monitoring the transient current decay for two hours. Cyclic voltammograms were then initiated by scanning cathodically from 0.4 to 0.2 V at a rate of 10 μV s^{-1}. Enzymes were quantified by integrating the cathodic peak in the CV. The resulting charge, Q, was converted to surface concentration by assuming four reducing equivalents per enzyme (for type 1, 2, and 3 copper centers in laccase) under anaerobic conditions.

RESULTS

Cathodic polarization of laccase-adsorbed ketjen black electrodes was performed between 0.6 and 0.0 V in pH 5.0 acetate buffer. Under these conditions, the onset of a catalytic current was observed at ca. 340 mV vs Ag|AgCl, with a limiting current observed by 0.0 V. Dependence of this catalytic wave on the presence of dioxygen was confirmed through experiments carried out under anaerobic conditions, which resulted in the disappearance of the wave (Figure 2, red curve). To establish an upper limit of the current that could be drawn from this system, studies of the current dependence on electrode rotation were conducted using an RDE setup. At lower speeds we observe a linear variance of the cathodic current density (j_L) with the square root of the rotation rate ($\omega^{1/2}$), as predicted by the Levich equation (eq 3):[14]

$$j_L = 0.62nFD^{2/3}\omega^{1/2}\nu^{-1/6}C \quad (3)$$

Higher angular velocities result in a loss of the linear relationship between current and rotation rates, as dioxygen flux to the cathodic surface stops being rate-limiting above 4000 rpm (Figure 2, inset). At this rotation speed, the catalytic current trends toward a plateau around 0.56 mA cm^{-2} under the stated conditions.

Quantitative evidence for the complete electrochemical transformation of O_2 to H_2O by *T. thermophilus* laccase was obtained by measuring the steady-state O_2 consumption of laccase under a constant applied potential (Figure 3a). By comparing the total amount of dioxygen consumed over a period of two hours to the total amount of charge passed through the system during the same time interval, we calculated a faradaic yield of 0.947 ± 0.023, indicating that approximately 95% of the dioxygen turned over by the enzyme results in water production. This outcome serves as a testament to the high catalytic specificity of this laccase variant, even when operating as a heterogeneous catalyst.

Despite a catalytic optimum of 95 °C reported for *T. thermophilus* laccase when acting upon organic substrates in solution, our studies revealed a catalytic optimum of only 55 °C for this enzyme when adsorbed onto modified ketjen black. By 80 °C, the electrode had lost most of its activity (Figure 3b). Laccase cathodes displayed reasonably good temporal stability during potentiostatic trials, retaining over 98% of their initial activity over the course of an hour at 30 °C when poised at a high (340 mV) overpotential (SI). Eyring analysis of *T. thermophilus* laccase thermal dependence reveals an activation enthalpy of 18.4 ± 2·2 kJ mol^{-1}, substantially lower than those reported for *Myrothecium verrucaria* (28.2 kJ mol^{-1}) and *Trachyderma tsunodae* (34.3 kJ mol^{-1}) laccases employed in similar electrode systems (Figure 3b, inset).[16] The optimal catalytic activity was observed at pH 5.0, with the enzyme exhibiting a linear dependence on proton concentration in the range pH 4.0−6.0, with a slope of 57 ± 1 mV $decade^{-1}$, a value close to the ideal slope of 59 mV for the pH dependence of a Nernstian, one-electron process (SI).[15]

Investigations of interfacial electron transfer processes were aided by Tafel analysis, which allowed for the determination of the equilibrium exchange current density (j_0), charge transfer resistance (Ω_{ct}), and the transmission frequency (α) of electron transfer between the type 1 copper site in laccase and the cathode surface. We find j_0 = 27.2 ± 3.7 μA cm^{-2} at 303 K and a corresponding Ω_{ct} of 3890 ± 518 ohms (Figure 4). Our system exhibits an α of 0.48 ± 0.05, which is highly suggestive

dx.doi.org/10.1021/jp309759g | J. Phys. Chem. B XXXX, XXX, XXX−XXX

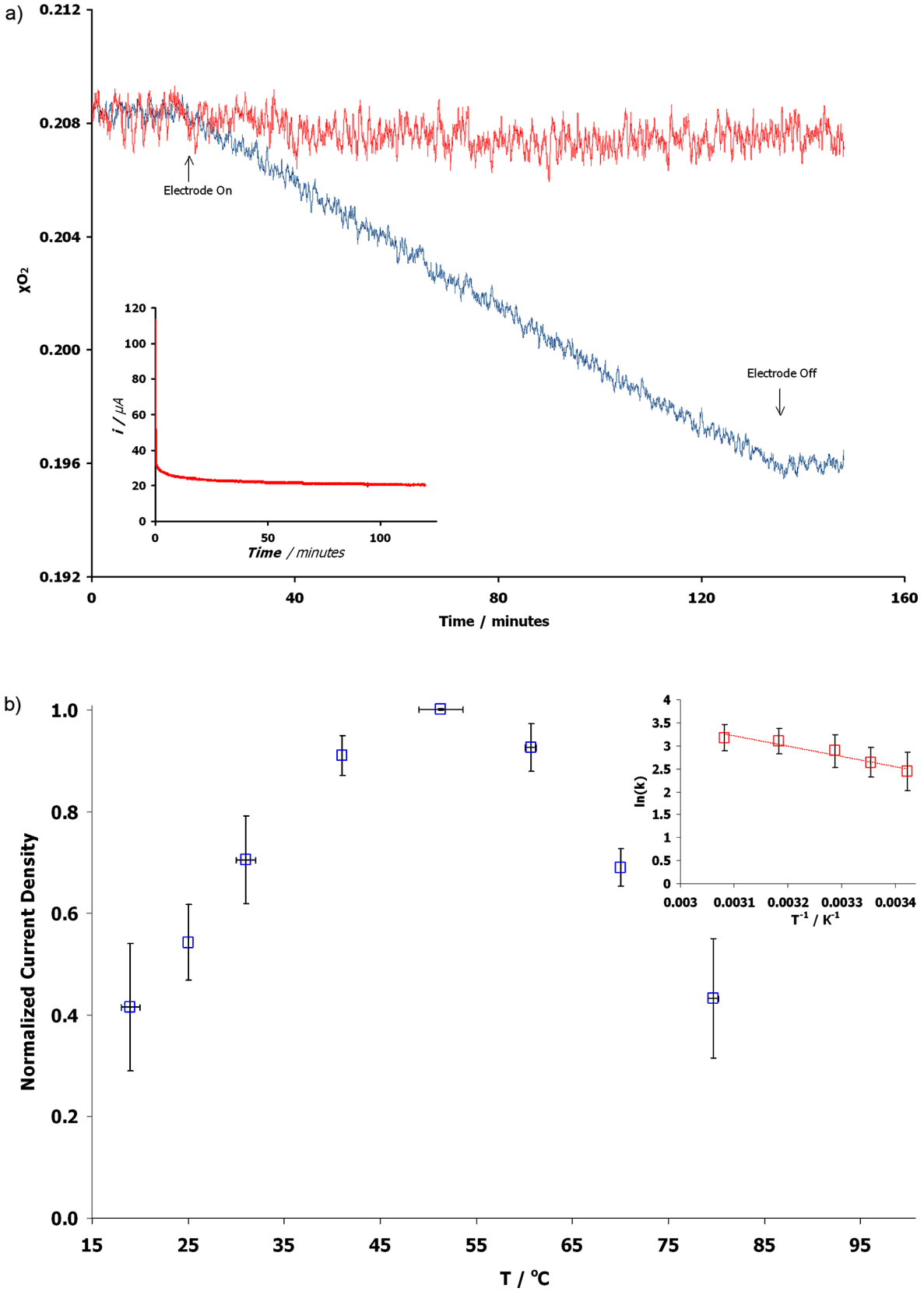

Figure 3. a. Faradaic yields for laccase electrocatalysis. Electrodes were poised at 0.0 V vs Ag|AgCl for two hours with concomitant monitoring of O_2 consumption. Dioxygen concentration of a cell operating with an enzyme-functionalized electrode is depicted in blue. Control electrodes (no enzyme) show no decrease in O_2 content over time (red trace). (inset) An amperometric trace of electrode current during the experiment. b. Temperature dependence of laccase activity in pH 5.0, 20 mM sodium acetate with electrode rotation at 3200 rpm. Inset: Eyring analysis reveals an activation energy of 18.4 ± 2.2 kj mol^{-1} for heterogeneous electrochemical O_2 reduction by *T. thermophilus* laccase (fitting equation: y = −2212.5x + 10.073; R^2 = 0.93).

dx.doi.org/10.1021/jp309759g | *J. Phys. Chem. B* XXXX, XXX, XXX−XXX

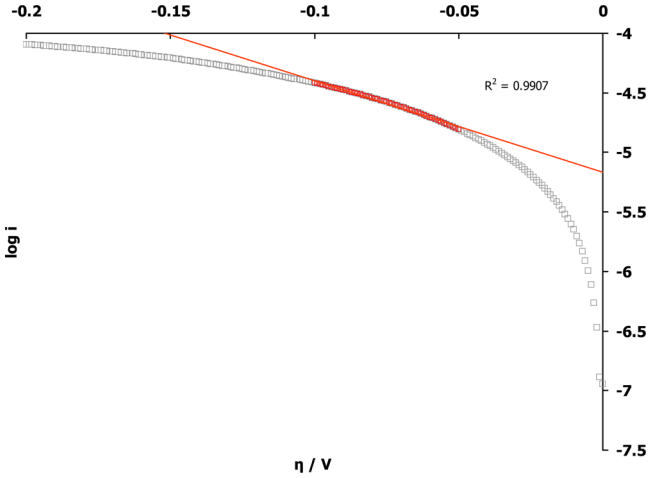

Figure 4. A typical cathodic Tafel branch of a laccase electrode scanned anodically in pH 5.0, 20 mM sodium acetate at 3000 rpm. Our fitting methodology predicts the 50−100 mV overpotential regime (highlighted in red) as the most appropriate region for conducting the linear analysis. Using this fit, extrapolation of the linear region to the point of zero driving force reveals an exchange current density of 27.2 μA cm^{-2}.

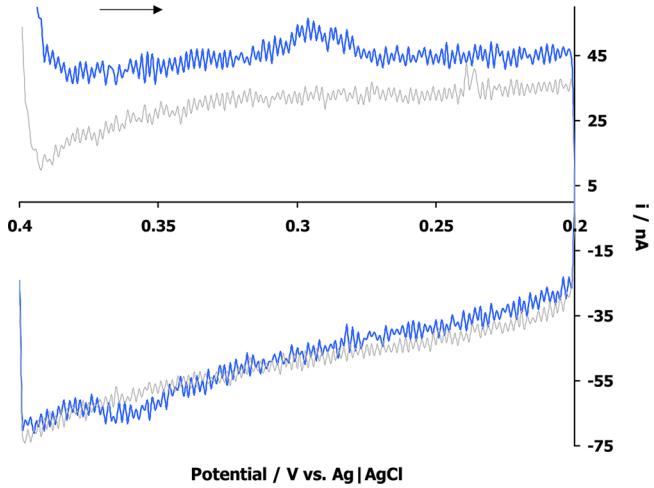

Figure 5. Cyclic voltammgram of a laccase-modified electrode under anaerobic conditions (blue trace) scanned from 0.4 to 0.2 V vs Ag|AgCl at 10 μV s^{-1} in pH 4.6 50 mM phosphate + 250 mM sulfate buffer. Peaks occur at 300 and 360 mV for the cathodic and anodic processes, respectively, and are assigned to sacrificial reduction and oxidation of the type I copper site in laccase. Peak integration provides a value of 25 μC, corresponding to 3.9 × 10^{13} electrochemically active enzymes on the ketjen substrate. Negative (no enzyme) controls show no peaks in the CV (gray trace) under virtually identical conditions. The black arrow signifies the start of the scan (cathodic direction).

of a symmetric Marcus coordinate, the situation expected for electron flow between a donor and acceptor in the zero-overpotential limit. The moderate Tafel slope of 128 ± 13.8 mV decade^{-1} is typical of this class of electrode and within error of the expected slope (~118 mV) of an ideal, one-electron transfer at ambient temperature, where α = 0.5.[15] Furthermore, this Tafel slope agrees well with the reported value of 145 mV decade^{-1} for *Trametes versicolor* laccase − modified gold cathodes and also bilirubin oxidase cathodes (120 mV decade^{-1}).[16,17]

Using voltammetry performed under strictly anaerobic atmospheres, we were able to quantify the amount of electrochemically active enzymes incorporated into our ketjen black electrodes through observation of peaks due to sacrificial reduction of the type 1 copper site in *Thermus thermophilus* laccase. Prior to running CVs, amperometric sweeps were run at 0.6 V under argon until the current decayed to zero, ensuring that at least the type 1 Cu sites in all electrochemically active enzyme centers were fully oxidized. CVs were then run starting in the cathodic direction at a rate of 10 μV s^{-1}. Peaks assigned to the reduction and oxidation of the type 1 active site occurred at 0.30 and 0.36 V, respectively (Figure 5). Integration under the cathodic peak yielded 25 ± 7 μC. Our use of amperometric oxidation prior to voltammetry prompted the assumption of a four-electron-per-enzyme stoichiometry when calculating the size of the electrochemically active enzyme population from the cathodic integral. This yields 3.9 ± 1.1 × 10^{13} functioning enzyme centers. We emphasize that the cathodic peak is far more ideal for this calculation than the anodic signal, since knowledge that the resting form of an MCO has all metal sites in the cupric state guarantees that during an anaerobic, cathodic scan, four equivalents of charge are taken up by the enzyme.[18]

The ability to probe both the surface concentration of electrochemically competent enzymes and the value of the equilibrium exchange current enabled us to calculate a k_{ET} value of 1.0 ± 0.3 s^{-1} for electron transport across the enzyme-electrode interface at zero driving force at 30 °C. Using values for the peak current achieved during temperature dependence studies (3200 rpm rotation), we estimate a k_{ET} of 16.2 ± 7.5 s^{-1} at 30 °C and a maximum rate constant of 22.7 ± 8.6 s^{-1} at 50 °C under an applied 240 mV overpotential during catalytic electrode operation.

DISCUSSION

We assign the current onset at ca. 340 mV vs Ag|AgCl to the reduction potential of the type 1 copper center of *T. thermophilus* laccase. This type 1 potential is considerably depressed relative to those of other high-potential laccase homologues and is far from the thermodynamic potential for the reduction of dioxygen to water, possibly owing to the short Cu-(S)Met axial bond in this enzyme, an interaction known to be critical for tuning type 1 copper reduction potentials.[16,18,19] A primary challenge posed by the cathodes designed for this study is that their peak current of 0.56 mA cm^{-2} is not only low compared to targets for fuel cells aimed at mobile applications (~100 mA cm^{-2}) but is also associated with a high (~240 mV) overpotential.[20] Furthermore, the longevity of these cathodes still needs to be improved for continuous use in devices running for several weeks or months.

The successful determination of faradaic yields for this electrochemical process indicates that *T. thermophilus* laccase is incredibly efficient at using dioxygen as an electron sink, with hardly any O_2 reduction intermediates resulting from catalytic turnover. Our result is consistent with findings for other MCOs, where high coulombic efficiencies have been inferred from studies employing methods such as rotating ring disk analysis to probe for O_2 reduction intermediates resulting from enzymatic turnover.[38,39]

The extracted interfacial rate constant of 1 s^{-1} represents an average rate for all centers in electrical contact with the electrode surface, as our passive adsorption method results in an ensemble of immobilized proteins of nonuniform orientation. For electron tunneling from a conductive surface through a peptide to a redox cofactor, this rate implies a

dx.doi.org/10.1021/jp309759g | J. Phys. Chem. B XXXX, XXX, XXX−XXX

relatively large average distance between the type 1 site and the electrode surface.[21−26] Estimating a reorganization energy between 0.3 and 1.0 eV for the type 1 site, a range encompassing reorganization in most type 1 centers,[27,28] places the average value of the electronic coupling (H_{ab}) between the type 1 copper and the electrode surface between 0.0002 and 0.008 cm^{-1}, respectively. It is of interest that the slow electron transfer in this system falls far below the interfacial rate constant that has been reported for an oriented enzyme electrode.[29]

The very slow scan rates employed during anaerobic voltammetry made it possible for us to resolve the noncatalytic peaks due to reduction of the type 1 copper sites in *T. thermophilus* laccase. We note that among the many studies conducted on MCOs functioning on ketjen black, and, more generally, substrates where enzymes are randomly oriented on high surface area materials, measurements of the interfacial ET rates are seldom reported. This recurring omission derives from the difficulty in determining the surface concentrations of electrochemically active enzymes adsorbed to electrode surfaces in these systems. This problem seems also to extend to other types of proteins passively adsorbed on electrode substrates, prompting rough quantification by nonelectrochemical methods such as atomic-force microscopy, transmission electron microscopy, or using very generalized approximations derived from catalytic polarization curves.[16,30,31] Some groups have suggested that the number of active enzyme centers on these electrodes is too small to probe with standard voltammetric techniques.[16] Although likely a contributing factor to the difficulty of surface measurement, rough estimations in the literature for concentrations of these enzymes on surfaces ($\sim 10^{12}-10^{13}$ centers cm^{-2}), coupled with the knowledge of the exchange current densities in these systems, allowed for our preliminary estimates of a k_{ET} between 0.1 and 10 s^{-1}.[16,30] These approximations suggested that performing voltammetry under scan rates traditionally used in protein electrochemistry (10−200 mV s^{-1}) may be too high to probe such slow electron transfer processes, prompting our work at much lower scan rates. We suggest that voltammetric sweeps at 10 μV s^{-1} are best suited for determining surface concentrations of electrochemically active species in a ketjen-MCO electrode assembly. We also note that while such slow sweep rates are unusual, they are not without precedent,[14] and, in fact, agree with the general rule that sweep rates should be limited according to eq 4

$$C_{DL}dv/dt \leq j_F \quad (4)$$

where C_{DL} is the dual-layer capacitance of a system of interest, the differential is the sweep rate, and j_F is the current density of the faradaic process of interest.[15] Our anaerobic scans reveal peak currents in the nanoampere regime; assuming prototypical dual-layer capacitances of 50−100 μF cm^{-2}, this relation predicts sweep rates of 10−20 μV s^{-1} as a prerequisite for their resolution from the background noise resulting from capacitive charging.[15] We regard this final point as additional validation of the methodology presented here.

Electron transfer between the electrode and the type 1 active site is the rate-limiting step in laccase electrocatalysis. In catalysis requiring charge transfer between sequential redox centers, only electron acceptors within electrical contact of the electrode should exhibit any sensitivity to the surface potential. In MCOs the type 1 site is such an acceptor. This view is corroborated both by the observations in MCO literature that the type 2/3 centers in these enzymes are too insulated to interact with either electrodes or small molecule redox mediators in solution chemistry and the higher rates of intramolecular ET that have been measured in laccase homologues using spectroscopic methods.[32−35]

CONCLUSION

The laccase homologue from the bacterium *Thermus thermophilus* strain HB27 is capable of catalyzing dioxygen reduction to water in a heterogeneous system with high faradaic yield. The system has a number of drawbacks, namely the low potentials where electrocatalysis is maximal and also the relatively small peak currents. However, we emphasize that many of these shortcomings can be addressed, either through improvements to the enzyme itself or the techniques used to fabricate the electrode assemblies. In particular, many studies have demonstrated the tunability of the type 1 copper center in a variety of blue copper proteins, yielding higher potential variants; most notable in this field is the large body of work that has been done on *Pseudomonas aeruginosa* azurin and CueO from *E. coli*.[19,28,36,37] We are currently seeking to enhance the electronic coupling by establishing enzyme monolayers of homogeneous orientation, with the type 1 center held proximal to the electrode surface. Assuming catalyst coverages reported here, the results of this study suggest that achieving H_{ab} values between ∼0.002 and 0.08 cm^{-1} would allow for realization of currents in the 60 mA cm^{-2} regime.

We report explicit quantification of the surface concentration of *active* laccase species on ketjen black using voltammetry, allowing for determination of the number of enzymes coupled to the electrode following adsorption to this high-surface area material. This, in turn, provided a rare opportunity to calculate the value of the heterogeneous rate constant for electron transfer between the electrode surface and an MCO active site on ketjen black. The small value of k_{ET} reported here indicates that interfacial charge transfer is rate-limiting in these systems and that its optimization should be the primary focus of any future attempts to increase the current densities of biological cathodes.

ASSOCIATED CONTENT

Supporting Information

Protein mass spectrum, circular dichroism, controlled-potential electrolysis, and pH dependence measurements. This material is available free of charge via the Internet at http://pubs.acs.org.

AUTHOR INFORMATION

Corresponding Author

*E-mail: hbgray@caltech.edu.

Notes

The authors declare no competing financial interest.

ACKNOWLEDGMENTS

We thank James Mckone, Alec Durrell, and Bryan Stubbert for helpful discussions regarding electrochemistry and Kyle Lancaster for discussions regarding biochemistry. This research was funded by GCEP (Stanford), CSER (The Gordon and Betty Moore Foundation), and NIH (DK019038). Additional support was provided by a partial fellowship from the Institute for Collaborative Biotechnologies through grant W911NF-09-0001 from the U.S. Army Research Office and the Department of Energy, Basic Energy Sciences (DE-FG03-01ER46175)(JRH PI).

REFERENCES

(1) Soukharev, V.; Mano, N.; Heller, A. *J. Am. Chem. Soc.* **2004**, *126*, 8368−8369.
(2) Carver, C. T.; Matson, B. D.; Mayer, J. M. *J. Am. Chem. Soc.* **2012**, *134*, 5444−5447.
(3) Roberts, S. A.; Weichsel, A.; Grass, G.; Thakali, K.; Hazzard, J. T.; Tollin, G.; Rensing, C.; Montfort, W. R. *Proc. Natl. Acad. Sci. U.S.A.* **2002**, *99*, 2766−2771.
(4) Komori, H.; Sugiyama, R.; Kataoka, K.; Higuchi, Y.; Sakurai, T. *Angew. Chem., Int. Ed.* **2012**, *51*, 1861−1864.
(5) Blanford, C. F.; Heath, R. S.; Armstrong, F. A. *Chem. Commun.* **2007**, *17*, 1710−1712.
(6) Miura, Y.; Tsujimura, S.; Kurose, S.; Kamitaka, Y.; Kataoka, K.; Sakurai, T.; Kano, K. *Fuel Cells* **2009**, *9*, 70−78.
(7) Miyazaki, K. *Extremophiles* **2005**, *9*, 415−425.
(8) Liu, X.; Gillespie, M.; Ozel, A. D.; Dikici, E.; Daunert, S.; Bachas, L. G. *Anal. Bioanal. Chem.* **2011**, *399*, 361−366.
(9) Tsujimura, S. *Electrochim. Acta* **2008**, *53*, 5716−5720.
(10) Blanford, C. F.; Foster, C. E.; Heath, R. S.; Armstrong, F. A. *Faraday Discuss.* **2008**, *140*, 319−335.
(11) Kataoka, K.; Hirota, S.; Maeda, Y.; Kogi, H.; Shinohara, N.; Sekimoto, M.; Sakurai, T. *Biochemistry* **2011**, *50*, 558−565.
(12) Cracknell, J. A.; Vincent, K. A.; Armstrong, F. A. *Chem. Rev.* **2008**, *108*, 2439−2461.
(13) Gallaway, J.; Wheeldon, I.; Rincon, R.; Atanassov, P.; Banta, S.; Barton, S. C. *Biosens. Bioelectron.* **2008**, *23*, 1229−1235.
(14) Bard, A. J.; Faulkner, L. R. *Electrochemical Methods: Fundamentals and Applications*; Wiley: 2001.
(15) Bockris, J. O.; Reddy, A. K. N.; Gamboa-Aldeco, M. *Modern Electrochemistry*; Springer: 2000.
(16) Thorum, M. S.; Anderson, C. A.; Hatch, J. J.; Campbell, A. S.; Marshall, N. M.; Zimmerman, S. C.; Lu, Y.; Gewirth, A. A. *J. Phys. Chem. Lett.* **2010**, *1*, 2251−2254.
(17) Mano, N.; Fernandez, J. L.; Kim, Y.; Shin, W.; Bard, A. J.; Heller, A. *J. Am. Chem. Soc.* **2003**, *125*, 15290−15291.
(18) Solomon, E. I.; Sundaram, U. M.; Machonkin, T. E. *Chem. Rev.* **1996**, *96*, 2563−2606.
(19) Lancaster, K. M.; George, S. D.; Yokoyama, K.; Richards, J. H.; Gray, H. B. *Nat. Chem.* **2009**, *1*, 711−715.
(20) Thomas, S. C.; Ren, X.; Gottesfeld, S.; Zelenay, P. *Electrochim. Acta* **2002**, *47*, 3741−3748.
(21) Gray, H. B.; Winkler, J. R. *Chem. Phys. Lett.* **2009**, *483*, 1−9.
(22) Gray, H. B.; Winkler, J. R. *Proc. Natl. Acad. Sci. U.S.A.* **2005**, *102*, 3534−3539.
(23) Gray, H. B.; Winkler, J. R. *Q. Rev. Biophys.* **2003**, *36*, 341−372.
(24) Gray, H. B.; Winkler, J. R. *Biochim. Biophys. Acta, Bioenerg.* **2010**, *1797*, 1563−1572.
(25) Edwards, P. P.; Gray, H. B.; Lodge, M. T. J.; Williams, R. J. P. *Angew. Chem., Int. Ed. Engl.* **2008**, *47*, 6758−6765.
(26) Onuchic, J. N.; Beratan, D. N.; Winkler, J. R.; Gray, H. B. *Annu. Rev. Biophys. Biomol. Struct.* **1992**, *21*, 349−377.
(27) Lancaster, K. M.; Farver, O.; Wherland, S.; Crane, E. J.; Richards, J. H.; Pecht, I.; Gray, H. B. *J. Am. Chem. Soc.* **2011**, *133*, 4865−4873.
(28) Hong, G.; Ivnitski, D. M.; Johnson, G. R.; Atanassov, P.; Pachter, R. *J. Am. Chem. Soc.* **2011**, *133*, 4802−4809.
(29) Udit, A. K.; Hill, M. G.; Bittner, V. G.; Arnold, F. H.; Gray, H. B. *J. Am. Chem. Soc.* **2004**, *126*, 10218−10219.
(30) Tamaki, T.; Hiraide, A.; Asmat, F. B.; Ohashi, H.; Ito, T.; Yamaguchi, T. *Ind. Eng. Chem. Res.* **2010**, *49*, 6394−6398.
(31) Kato, M.; Cardona, T.; Rutherford, A. W.; Reisner, E. *J. Am. Chem. Soc.* **2012**, *134*, 8332−8335.
(32) Farver, O.; Pecht, I. *Proc. Natl. Acad. Sci.* **1992**, *89*, 8283−8287.
(33) Farver, O.; Wherland, S.; Koroleva, O.; Loginov, D. S.; Pecht, I. *FEBS J.* **2011**, *278*, 3463−3471.
(34) Farver, O.; Wherland, S.; Pecht, I. *J. Biol. Chem.* **1994**, *269*, 22933−22936.
(35) Simaan, A. J.; Mekmouche, Y.; Herrero, C.; Moreno, P.; Aukauloo, A.; Delaire, J. A.; Réglier, M.; Tron, T. *Chem.—Eur. J.* **2011**, *17*, 11743−11746.
(36) Sakurai, T.; Kataoka, K. *Cell. Mol. Life Sci.* **2007**, *64*, 2642−2656.
(37) Sheng, Y.; Wang, W.; Chen, P. *J. Mol. Struct.* **2011**, *995*, 142−147.
(38) Tonda-Mikiela, P.; Habrioux, A.; Boland, S.; Servat, K.; Tingry, S.; Kavanagh, P.; Napporn, T. W.; Leech, D.; Kokoh, K. B. *Electrocatalysis* **2011**, *2*, 268−272.
(39) Scodeller, P.; Carballo, R.; Szamocki, R.; Levin, L.; Forchiassin, F.; Calvo, E. J. *J. Am. Chem. Soc.* **2010**, *132*, 11132−11140.